

## The LHCb VERTEX LOCATOR performance and VERTEX LOCATOR upgrade

This article has been downloaded from IOPscience. Please scroll down to see the full text article.

2012 JINST 7 C12008

(<http://iopscience.iop.org/1748-0221/7/12/C12008>)

View [the table of contents for this issue](#), or go to the [journal homepage](#) for more

Download details:

IP Address: 193.144.83.51

The article was downloaded on 17/12/2012 at 09:14

Please note that [terms and conditions apply](#).

14<sup>th</sup> INTERNATIONAL WORKSHOP ON RADIATION IMAGING DETECTORS,  
1–5 JULY 2012,  
FIGUEIRA DA FOZ, PORTUGAL

## The LHCb VERTEX LOCATOR performance and VERTEX LOCATOR upgrade

---

**P. Rodríguez Pérez**<sup>1,2</sup>

*University of Santiago de Compostela,  
Santiago de Compostela, Spain*

*E-mail: [pablo.rodriguez@usc.es](mailto:pablo.rodriguez@usc.es)*

**ABSTRACT:** LHCb is an experiment dedicated to the study of new physics in the decays of beauty and charm hadrons at the Large Hadron Collider (LHC) at CERN. The Vertex Locator (VELO) is the silicon detector surrounding the LHCb interaction point. The detector operates in a severe and highly non-uniform radiation environment. The small pitch and analogue readout result in a best single hit precision of 4  $\mu\text{m}$ .

The upgrade of the LHCb experiment, planned for 2018, will transform the entire readout to a trigger-less system operating at 40 MHz event rate. The vertex detector will have to cope with radiation levels up to  $10^{16}$   $1 \text{ MeVn}_{\text{eq}}/\text{cm}^2$ , more than an order of magnitude higher than those expected at the current experiment. A solution is under development with a pixel detector, based on the Timepix/Medipix family of chips with  $55 \times 55 \mu\text{m}$  pixels. In addition a micro-strip solution is also under development, with finer pitch, higher granularity and lower mass than the current detector. The current status of the VELO will be described together with recent testbeam results.

**KEYWORDS:** Particle tracking detectors; Si microstrip and pad detectors

---

<sup>1</sup>Corresponding author.

<sup>2</sup>On behalf of the LHCb VELO Group and the VELO Upgrade group.

---

## Contents

<b>1</b>	<b>The VELO detector at the LHCb experiment</b>	<b>1</b>
1.1	The LHCb experiment	1
1.2	The VERTEX LOCATOR (VELO)	1
1.3	VELO performance	2
1.4	Radiation damage	2
<b>2</b>	<b>The VELO upgrade</b>	<b>3</b>
2.1	The LHCb upgrade	3
2.2	The VELO upgrade	4
2.3	The testbeam program	6
<b>3</b>	<b>Conclusions</b>	<b>7</b>

---

## 1 The VELO detector at the LHCb experiment

### 1.1 The LHCb experiment

LHCb [1] is an experiment with forward geometry and has shown excellent vertex, momentum and particle identification capabilities. LHCb has recorded for analysis  $1.0 \text{ fb}^{-1}$  pp collisions at 7 TeV center of mass energy during 2011. After 2011-2012 winter shutdown the energy was increased to 8 TeV, and since then,  $1.4 \text{ fb}^{-1}$  have been recorded (September 2012). Currently LHCb is running at a luminosity of  $\mathcal{L} = 4 \times 10^{32} \text{ cm}^{-2} \text{ s}^{-1}$  with an average pile up of 1.4 interactions per bunch crossing. Both values are above design values, which is an indication of the excellent performance of the experiment.

### 1.2 The VERTEX LOCATOR (VELO)

The Vertex Locator (VELO) [2] is the silicon detector surrounding the LHCb interaction point. It is located only 7 mm from the beams during normal operation and measures very precisely the primary vertex and the decay vertices. It consists of two retractable detector halves with 21 silicon micro-strip tracking modules each (figure 1). A module is composed of two  $n^+$ -on-n  $300 \mu\text{m}$  thick half disc sensors with R and  $\phi$ -measuring micro-strip geometry. The detector is operated in vacuum and a bi-phase  $\text{CO}_2$  cooling system is used. The sensors are readout with the analogue front-end chip (Beetle [3]).

Only when the stable beam flag is raised both halves of the VELO are closed, allowing a small overlap in the inner region, reaching a distance of only 7 mm to the beam line.

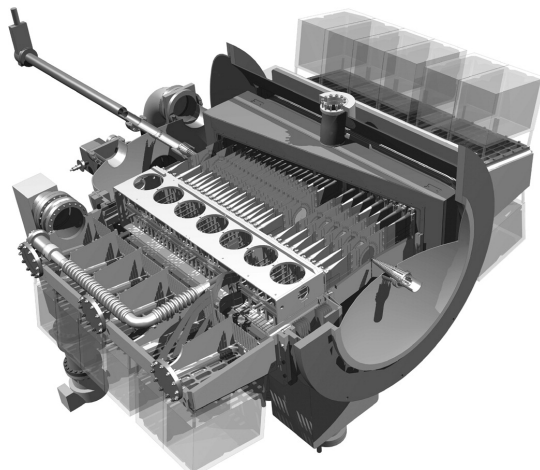


**Figure 1.** CAD image of the VELO detector. The beam pass through the center of the detector where the collisions occur.

### 1.3 VELO performance

The 1 MHz L0 trigger rate is reduced to a few kHz by full event reconstruction in the computer farm. The VELO plays a crucial role providing vertexing information for this decision. On the tracking and vertexing side, the VELO provides accurate reconstruction of primary and decay vertices, reaching a point resolution of  $4\ \mu\text{m}$  in the  $40\ \mu\text{m}$  pitch region at optimal angle ( $\sim 10^\circ$ , figure 2(a)). The primary vertex resolution (PV) is  $13\ \mu\text{m}$  in the longitudinal direction for about 25 tracks (figure 2(b)). The final momentum dependent impact parameter resolution (IP) is  $11.5 + 24.5/p_T$ , where  $p_T$  is the transverse momentum in  $\text{GeV}/c$  (figure 2(c)). Accurate determination of the IP is very important for LHCb. The relationship between the IP and the PV for a particle is used in the trigger as cut in many physics analysis.

As result, a lifetime resolution of  $\sim 50\ \text{fs}$  was achieved for the flagship channel  $B_s \rightarrow J/\psi\phi$  [4], typical of those channels where the resolution is necessary to resolve fast  $B_s$  oscillations. Excellent resolution is also very important for background suppression in rare decay channels.

### 1.4 Radiation damage

Due to the small distance to the interaction point severe radiation damage is foreseen in the VELO sensors [5], with doses  $\sim 0.6 \times 10^{14} \text{MeVn}_{\text{eq}}\text{cm}^{-2}$  per accumulated  $\text{fb}^{-1}$ . The increase of the leakage current was measured as a function of the delivered luminosity (see figure 3(a)). The periods with a decrease in the current corresponds to the annealing during shutdown periods or to occasional detector warm ups. The typical current increase is around  $1.9\ \mu\text{A}$  per  $100\ \text{pb}^{-1}$  delivered. The effective depletion voltage is measured with HV scans during dedicated datataking periods. Figure 3(b) displays the results of these scans split by detector region and received dose. Most of the innermost parts of the  $n^+$ -on- $n$  sensors have already passed through type inversion. Studies of the cluster finding efficiency have revealed a radiation induced charge loss in R-type sensors. For these sensors the mean of the collected charge is lower, and the distribution has experienced deformation due to a growing fraction of clusters with very small charge. The effect has been linked to coupling between routing lines in the second metal layer and the aluminium

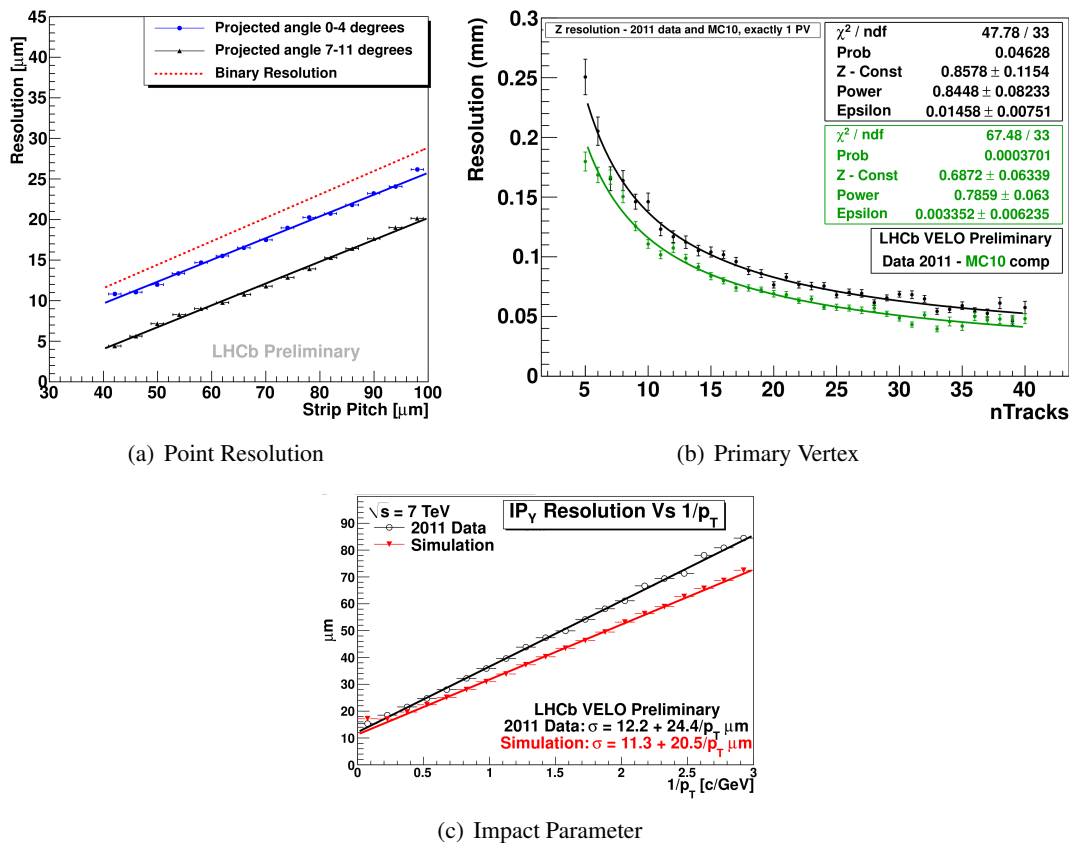


**Figure 2.** Figure (a) shows the single hit resolution of R-sensors as function of strip pitch for two different projected angles. The binary resolution is shown as reference. Figure (b) shows the vertex resolution along the beam axes (Z) as function of the number of tracks. Figure (c) shows the impact parameter at optimal angle.

of the strips in the first metal layer. After irradiation, phantom signals in the inner strips (with readout through lines in the second metal layer) have been detected when the particles cross the outer strips. In the case of the  $\phi$  sensors the effect is mitigated because lines in both metalizations are collinear. The exact mechanism and the relationship with radiation damage is under study. For more information about radiation damage in the VELO, see [6, 7].

## 2 The VELO upgrade

### 2.1 The LHCb upgrade

The LHCb experiment will record around  $1\text{-}2 \text{ fb}^{-1}$  of data per year until end 2017, accumulating in excess of  $5 \text{ fb}^{-1}$ . Afterwards many of the physics channels will still be statistically limited. The LHC is already capable of delivering much higher luminosity to the experiment than the current one, therefore the LHCb has planned an upgrade for 2018 which is independent, but compatible with, the LHC upgrade. After the upgrade the experiment will operate at luminosities up to  $2 \times 10^{33} \text{ cm}^{-2} \text{ s}^{-1}$  and will readout collisions at 40 MHz. In these new conditions we expect to collect more than  $5 \text{ fb}^{-1}$  per year, with improvements of up to a factor 2 in the efficiencies in hadronic channels.

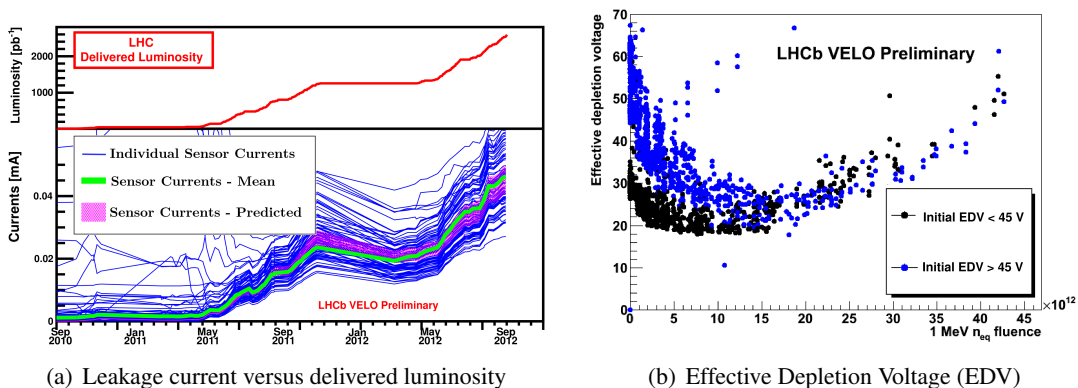


**Figure 3.** Radiation effects on VELO. Left plot shows the measured leakage current at  $-8^{\circ}\text{C}$  as function of the luminosity. Each blue line corresponds to a single sensor, the green curve is the mean current value excluding those sensors with initial high currents, and the pink band corresponds to predicted currents. The effective depletion voltage (EDV) for different sensors is shown in left plot. Blue dots corresponds to sensors with initially lower leakage currents, and black to sensors with high leakage current at the beginning.

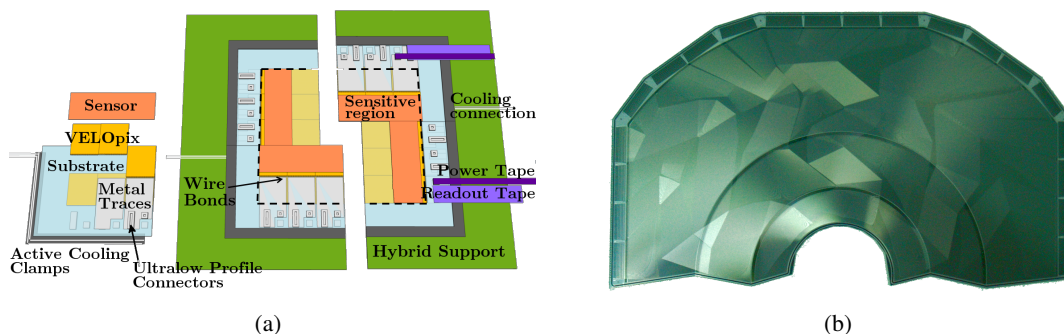


**Figure 4.** L-shape module for the pixel prototype 4(a), and prototype of  $\phi$  strip sensor produced by Hamamatsu 4(b)

## 2.2 The VELO upgrade

It is a big challenge for the VELO to cope with the requirements of the LHCb upgrade, specially in terms of radiation damage and data bandwidth [8, 9]. These new conditions must be satisfied keeping, or improving, the performance of the current VELO in terms of precision, pattern recognition and impact parameter resolution. Many systems of the current VELO detector, such as the motion system, the vacuum, the power systems (LV/HV) and the evaporative  $\text{CO}_2$  cooling system, will be reused.

On the sensor side two options are under consideration, pixel sensors with an ASIC based on Medipix/Timepix family (figure 4(a)), and strips sensors with a new and more advanced ASIC (figure 4(b)). Both options imply a completely new module and RF Foil design.

**Requirements:** one of the main constraints for the VELO upgrade is the bandwidth associated to a triggerless experiment, specially with the increase of the luminosity. The total data rate coming out from the detector will be around 2.4 Tbit/s for the strip option, or 2.8 Tbit/s for the pixel option. The other main issue is the radiation damage, as the upgraded VELO must be able to withstand radiation levels above 400 MRad or  $10^{16}$   $1 \text{ MeV } n_{\text{eq}}/\text{cm}^2$ .

**Table 1.** Main Velopix features.

Pixel array	$256 \times 256$
Pixel size	$55 \mu\text{m} \times 55 \mu\text{m}$
Minimum threshold	$\sim 500 e^-$
Peaking time	$< 25 \text{ ns}$
Time walk	$< 25 \text{ ns}$
Measurements	Time-of-Arrival & Time-over-Threshold
ToT range	4 bit (1-2 MIP)
ToA resolution / range	25 ns / 12 bit
Count rate	Up to 500 Mhit/s/chip
Readout	Continuous, sparse, on-chip clustering
Output bandwidth	$> 12 \text{ Gbit/s}$
Power consumption	$< 3 \text{ W/chip}$
Radiation hardness	$> 500 \text{ MRad}$ , SEU tolerant

**FE Electronics:**

**Pixel option.** The baseline choice for the upgraded VELO is a pixel ASIC called Velopix, which is based on the Timepix3 [10]. Some of the Velopix characteristics are summarized in table 1. The ASIC will integrate local intelligence at the pixel level for time-over-threshold measurement and sparse readout, on-chip zero suppression and packet-based readout. In addition, Velopix must be immune to single-event upsets in its digital logic. The main difference between TimePix3 and Velopix is that the latter should cope with higher particle flux, hence the bandwidth must be 6 or 7 times greater. The Medipix3 family was designed to be radiation hard, and the Velopix chip will inherit this feature to cope with radiation conditions of the upgraded VELO.

**Strips option.** The backup solution is the strip sensor with an enhanced design and read-out chip. The development of the ASIC is ongoing in synergy with other silicon detectors in LHCb. It will implement embedded solutions such as clustering, sparsification, common mode suppression and pedestal subtraction. A strip design results in a lower material budget than a pixel based solution.

**Sensors:** the baseline option for the sensor is planar silicon with  $n^+$  type readout [11]. The challenges for both pixels and strips include coping with a large and very non uniform radiation dose, reducing the material budget and incorporating as narrow as possible guard rings.

For the strip option, sensors should have a minimum pitch of  $30 \mu\text{m}$  or below (currently  $40 \mu\text{m}$ ),  $200 \mu\text{m}$  thickness (currently  $300 \mu\text{m}$ ),  $n\text{-on-p}$  type, and with a variable pitch in order to keep the same occupancy per strip. For this option, several prototypes with R and  $\phi$  design were produced by Hamamatsu, and are currently under characterization in the University of Santiago de Compostela.

In the case of the pixel option, other alternatives than planar sensors are under consideration, like 3D sensors [12] and diamond sensors. Several 3D sensors from CNM were studied during last testbeam campaigns.

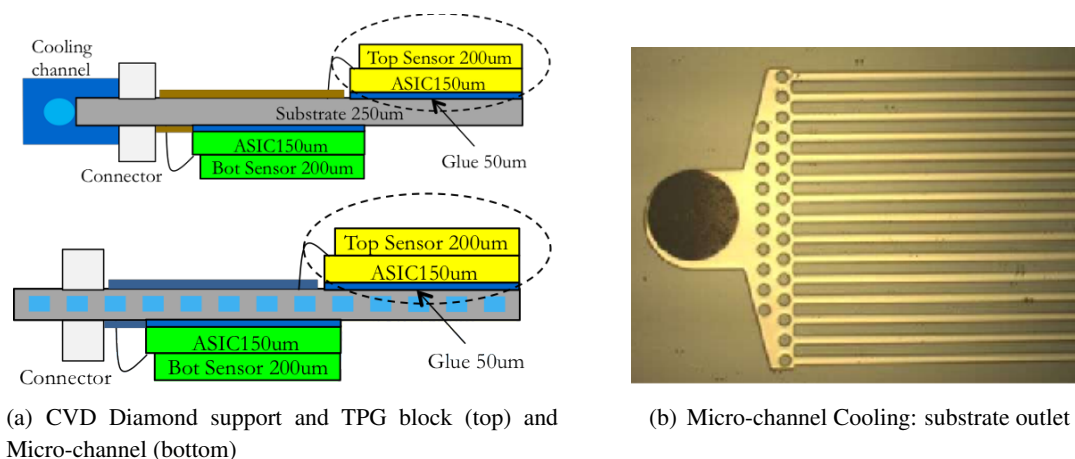


**Figure 5.** The two options under consideration for module cooling. Figure (a) (top) is the baseline solution based in a diamond support. Figures (a) (bottom) and (b) show the alternative solution based on microchannels etched into the silicon module's support. Microchannels dimensions are  $200\ \mu\text{m} \times 70\ \mu\text{m}$ .

**Mechanics and cooling:** as it was explained in section 2.2 the cooling system for the VELO upgrade will be based on the same evaporative  $\text{CO}_2$  system that is installed in the current VELO. However, two main techniques are being investigated in order to cool the module sensors.

**CVD Diamond.** A proposed solution (figure 5(a) top), and consists of a chemical vapor deposition (CVD) diamond support plus a thermal pyrolytic (TPG) cooling block. The diamond support guarantees a high thermal conductivity, highly robust and low material budget. For this solution the R&D is currently centered on diamond metalization.

**Micro-channel.** Through etching processes, a set of micro-channels are developed into a silicon substrate [13, 14]. The coolant ( $\text{CO}_2$ ) is forced to circulate through them at a pressure of  $\sim 60$  bar (figures 5(a)-bottom and 5(b)). It is an attractive solution because the channel layout can be adapted to the heat dissipation needs.

**RF-Foil:** the RF-Foil is the box that encloses the detector halves in a secondary vacuum. It is customized for the sensor layout to allow the placement of sensitive areas at the required distance from the beams, while slightly overlapping in closed configuration. The production of the new RF-Foil is ongoing with milling techniques, and a prototype has been produced for L-shape modules, which is the module for the pixel option. A large R&D is under way to manufacture a full scale prototype within the required specifications.

### 2.3 The testbeam program

We have built a testbeam telescope with 9 Timepix sensors [15], 8 in ToT<sup>1</sup> configuration and the last one in ToA.<sup>2</sup> This telescope has a point resolution at the Device Under Test (DUT) level of  $\sim 1.5\ \mu\text{m}$ , a time tag resolution of  $\sim 1$  ns and handles a track rate  $\approx 10$  kHz. The Timepix hybrids

<sup>1</sup>Time over Threshold provides a value proportional to the deposited energy.

<sup>2</sup>Time of Arrival provides the time-stamping of the track.

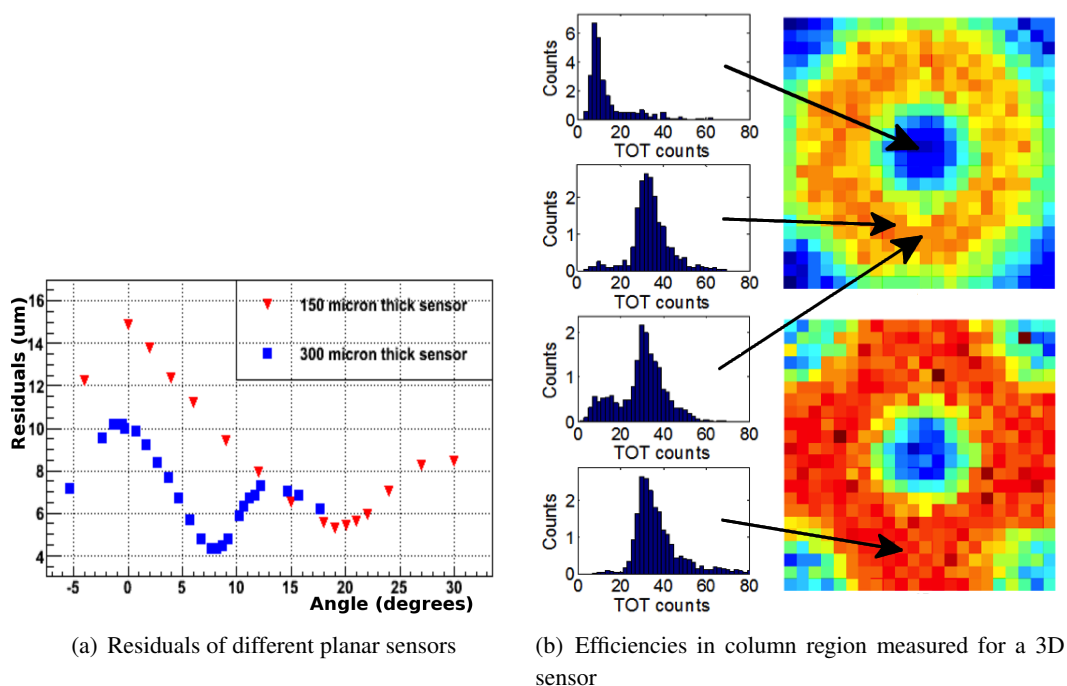


**Figure 6.** Figure (a) shows a comparison between two planar sensors of different thickness. Figure (b) shows the energy collected for a 3D sensor in a column neighborhood.

are connected to an innovative system called RELAXed which is based on FPGAs and can read 4 hybrids in parallel sending the data through an Ethernet connection.

Up to 8 different DUTs were analyzed with this telescope such as irradiated Medipix2 chips, thinned planar sensors (150  $\mu\text{m}$  thick) or 3D sensors [16]. In figure 6(a) a comparison between two planar sensors of 150  $\mu\text{m}$  and 300  $\mu\text{m}$  thickness is shown. The residual value inform us about the resolution of the reconstructed cluster in the DUT with respect to the extrapolated track given by the telescope, and it changes with the angle and the thickness as expected. In 3D sensors polarization is made between n-type and p-type columns etched into the silicon. Due to this particular geometry, a certain loss of efficiency is expected when a particle crosses the sensor trough a polarization column, as it can be seen in figure 6(b).

### 3 Conclusions

The VELO is operating smoothly under conditions beyond its design. It is a key element in the physics output of the LHCb due to its exceptional performance in terms of vertex and impact parameter resolutions.

As a consequence of the high radiation doses, the VELO sensors have already exhibited radiation damage, and type inversion is observed in the inner regions of the sensors. Nevertheless, the impact in the performance of the detector is not significant up to date.

In 2018 an upgrade of the VELO is planned that should be able to cope with the new requirements of the upgraded LHCb in terms of radiation hardness and readout bandwidth.

Some R&D is still needed in order to select the sensor technology and cooling for the upgraded detector. The candidates are pixels or strips with their associated FE electronics for the sensor and metallized diamond or microchannel for the cooling. The goal is to have confident technologies before 2014 when the production stage will start.

## References

- [1] LHCb collaboration, *The LHCb detector at the LHC*, [2008 JINST 3 S08005](#).
- [2] M. van Beuzekom, *Status and prospects of the LHCb vertex locator*, [Nucl. Instrum. Meth. A 596 \(2008\) 21](#).
- [3] S. Löchner and M. Schmelling, *The Beetle reference manual — Chip version 1.3, 1.4 and 1.5*, [CERN-LHCb-2005-105](#) (2006).
- [4] G. Krocker, *CP violation in  $B_s^0$  mixing with LHCb*, [arXiv:1112.0868](#).
- [5] J. Harrison and A. Webber, *Radiation damage in the LHCb VELO*, submitted to *Nucl. Instrum. Meth. A* (2012).
- [6] T. Affolder et al., *Use of IT (current vs. temperature) scans to study radiation damage in the LHCb VELO*, [CERN-LHCb-PUB-2011-021](#) (2011).
- [7] P. Rodriguez Perez, *LHCb: Radiation Damage in the LHCb VELO*, [Poster-2012-240](#) (2012).
- [8] P. Collins et al., *The LHCb VELO upgrade*, [Nucl. Instrum. Meth. A 636 \(2011\) S185](#).
- [9] P. Collins, *The LHCb VELO (Vertex Locator) and the LHCb VELO upgrade*, submitted to *Nucl. Instrum. Meth. A* (2012).
- [10] X. Llopart Cudié et al., *Timepix, a 65k programmable pixel readout chip for arrival time, energy and/or photon counting measurements*, [Nucl. Instrum. Meth. A 581 \(2007\) 485](#).
- [11] G. Casse et al., *Enhanced efficiency of segmented silicon detectors of different thicknesses after proton irradiations up to  $1 \times 10^{16} n_{eq} cm^{-2}$* , [Nucl. Instrum. Meth. A 624 \(2010\) 401](#).
- [12] G. Pellegrini et al., *3D double sided detector fabrication at IMB-CNM*, [Nucl. Instrum. Meth. A 699 \(2013\) 27](#).
- [13] A. Nomerotski et al., *Evaporative CO<sub>2</sub> cooling for upgraded LHCb VELO detector using microchannels etched in silicon*, submitted to *Nucl. Instrum. Meth. A* (2012) [[arXiv:1211.1176](#)].
- [14] A. Mapelli et al., *Microfluidic cooling for detectors and electronics*, [2012 JINST 7 C01111](#).
- [15] K. Akiba et al., *Charged particle tracking with the Timepix ASIC*, [Nucl. Instrum. Meth. A 661 \(2012\) 31](#) [[arXiv:1103.2739](#)].
- [16] K. Akiba et al., *Precision scans of the Pixel cell response of double sided 3D Pixel detectors to pion and X-ray beams*, [2011 JINST 6 P05002](#).